International Journal of Fatigue 100 (2017) 502–511

Contents lists available at ScienceDirect

International Journal of Fatigue

journal homepage: www.elsevier.com/locate/ijfatigue

Non-linear incremental fatigue damage calculation for multiaxial non-proportional histories

Marco Antonio Meggiolaro [a,*], Jaime Tupiassú Pinho de Castro [a], Hao Wu [b]

[a] Department of Mechanical Engineering, Pontifical Catholic University of Rio de Janeiro, Rua Marquês de São Vicente 225 – Gávea, Rio de Janeiro, RJ 22451-900, Brazil
[b] School of Aerospace Engineering and Applied Mechanics, Tongji University, 1239 Siping Road, Shanghai, PR China

ARTICLE INFO

Article history:
Received 15 September 2016
Received in revised form 11 November 2016
Accepted 3 December 2016
Available online 5 December 2016

Keywords:
Multiaxial fatigue
Variable amplitude load
Non-proportional multiaxial load
Nested fatigue damage surface
Incremental damage calculation

ABSTRACT

Most fatigue models must somehow identify and count individual load events before quantifying the damage induced by each one of them, making multiaxial fatigue damage calculations under non-proportional variable amplitude loadings a challenging and laborious task in practical applications. Moreover, to apply such models it is usually necessary to use semi-empirical methods to evaluate the non-proportionality of the load path of each event, through path-equivalent ranges obtained e.g. using a convex enclosure or the MOI (Moment Of Inertia) method. To avoid this burden, a new approach called the Incremental Fatigue Damage methodology is proposed in this work to continuously accumulate multiaxial fatigue damage under actual service loads, without requiring path-equivalent range estimators or rainflow counters. This new approach is not based on questionable Continuum Damage Mechanics concepts, or on the integration of some unrealistic scalar damage parameter based on elastoplastic work. Instead, inspired on multiaxial plasticity procedures, a framework of nested damage surfaces is introduced, allowing the calculation of fatigue damage even for general 6D multiaxial load histories. In this way, fatigue damage itself can be continuously integrated along the load path, considering damage parameters adopted by traditional fatigue models and following reliable procedures well tested in engineering practice. The proposed approach is experimentally validated by non-proportional tension-torsion tests on tubular 316L stainless steel specimens.

1. Introduction

Macroscopically speaking, fatigue damage can be regarded as a continuous process caused in real time by cyclic elastoplastic straining, usually localized in a single point of the structural component. To quantify such a process, most fatigue crack initiation models need to identify individual load cycles to compute the damage induced at that critical point by each one of them. In this way, such models require knowledge of the whole loading sequence to assess damage induced by the current event. So they are discrete in nature, since they can accumulate fatigue damage D only after a full cycle or half-cycle is identified, detected e.g. from a load reversal or from a hysteresis loop that closes.

Cycle identification under variable amplitude loading (VAL) is not a major problem under uniaxial (or proportional) load histories, since the rainflow method is an appropriate and sufficient cycle counting algorithm in this case [1]. But cycle detection and counting can be a quite challenging task under multiaxial non-proportional (NP) histories, where peaks/valleys of each stress or strain component in general do not coincide with the peaks/valleys of the other components. In this case, it is impossible to decide *a priori* which points should be considered as load reversals for cycle detection.

A simplistic approach [2] involves the application of a uniaxial rainflow count to one stress or strain component that can be assumed dominant in the multiaxial load history, assuming the others as secondary. This approach might be appropriate for quasi-proportional loadings, but under general NP VAL it will probably miss important load events in the secondary stress or strain components. Indeed, the peaks and valleys of the stresses and strains usually do not coincide, even if they act in the same direction, not to mention if they involve different stress or strain components. In such cases, a truly multiaxial rainflow algorithm that considers all stress or strain components must be adopted [3].

A number of multiaxial rainflow algorithms have been proposed in the literature. They are either based on cycle counting of von Mises equivalent stresses or strains such as the Wang-Brown, Modified Wang-Brown or Path-Dependent Multiaxial Rainflow

* Corresponding author.
E-mail addresses: meggi@puc-rio.br (M.A. Meggiolaro), jtcastro@puc-rio.br (Jaime Tupiassú Pinho de Castro), wuhao@tongji.edu.cn (H. Wu).

http://dx.doi.org/10.1016/j.ijfatigue.2016.12.008
0142-1123/

Nomenclature

CAL	constant amplitude loading
CDM	continuum damage mechanics
D	fatigue damage
D_σ or D_ε	generalized damage moduli with respect to stress or strain increments
EI	energy integration
$\vec{e}'$	deviatoric strain vector in the 5D deviatoric space
EP	elastic-plastic
EVICD	event independent cumulative damage
IDD	integration of damage differentials
IFD	incremental fatigue damage
LE	linear elastic
m_i	multiaxial ratcheting exponent of each hardening surface i
$\vec{n}'_\sigma$ or $\vec{n}'_\varepsilon$	normal unit vector in 5D deviatoric stress or strain spaces
N	fatigue life (in number of cycles)
NLDA	non-linear damage accumulation
NLK	non-linear kinematic
NP	non-proportional
$r_{\sigma i}$ or $r_{\varepsilon i}$	radius of each damage surface i in 5D deviatoric stress or strain spaces
$\vec{s}'$	deviatoric stress vector in the 5D deviatoric spaces
$\vec{v}'_{\sigma i}$ or $\vec{v}'_{\varepsilon i}$	surface translation directions in 5D deviatoric stress or strain spaces
VAL	variable amplitude loading
$\vec{\beta}'_{\sigma i}$ or $\vec{\beta}'_{\varepsilon i}$	damage surface backstresses in 5D deviatoric stress or strain spaces
σ_a	stress amplitude
$\chi_{\sigma i}$ or $\chi_{\varepsilon i}$	ratcheting exponent of each damage surface i for stress or strain spaces

methods [4–6], or on cycle counting of shear or normal stress (or strain) components acting on candidate planes from the critical-plane approach [7]. In the former case, cycles are identified in an effort to maximize the von Mises ranges between pairs of 6D stress (or strain) states, not necessarily maximizing damage since mean/maximum-stress effects are neglected in this search. In the latter case, a uniaxial rainflow is enough to count a single projected normal stress (or strain) component, but a 2D multiaxial rainflow is needed to combine both in-plane and out-of-plane shear components acting on the candidate plane. However, these 2D rainflow methods [3,5] for the critical-plane approaches unfortunately do not take into account mean/maximum-stress effects either. Critical plane criteria formulated on the frequency (instead of time) domain have been proposed too, but their accuracy is also affected by the uncertainty related to the algorithm used to count loading cycles [8]. Besides, the time to frequency transformation spoils the loading order sequence, losing in this way the capacity to model one of the most important features of fatigue loads, namely the memory effects associated with plastic events.

Moreover, the existing multiaxial rainflow algorithms are neither very robust nor consistent, since they can output very different half-cycles depending on the choice of the initial counting point of a periodic load history. Very complex multiaxial NP VAL histories may also be fragmented into too many half-cycles that might lead to non-conservative fatigue life predictions, by missing larger embedded cycles that are not accounted for. Furthermore, fatigue damage computation requires the calculation of path-equivalent stress or strain ranges from the rainflow-counted paths. Convex enclosure methods and the very efficient MOI method have been adopted for this purpose [9]. Although these methods have been proven effective for simple periodic loadings, they are phenomenological routines that might have issues with non-periodic multiaxial NP loadings with highly variable amplitudes or overloads. In summary, most fatigue damage calculation routines require methods for cycle identification, counting, and path-equivalent range computation, but no universal algorithms are so far available in the literature for properly dealing with complex NP multiaxial histories.

A completely different calculation approach is followed in this work, assuming fatigue damage is a continuous variable, whose increments can be computed as the loading proceeds. Fatigue damage is continuously calculated after each infinitesimal stress or strain increment, thus it does not need the identification of load cycles. In this way, this continuous fatigue damage approach does not require rainflow counting or path-equivalent range computations to deal with complex multiaxial loads.

However, beware that not all methods based on incremental damage parameters overcome the need for identifying load cycles: e.g. some creep-fatigue interaction models [10–13] consider continuous variations of damage, but they still require either well-defined cycles (cycle-based damage rules), or detection of load reversals (which are ill-defined for NP multiaxial loadings). Other creep-fatigue models provide time-incremental damage rules without considering any load reversal, but they are unable to correctly predict cyclic damage [13]. Thus, to correctly account for cyclic damage without requiring cycle detection, stress or strain-incremental damage rules must be adopted.

Dang Van's pioneer multiaxial fatigue criterion is a good example of a cycle-independent model [14], but it is only applicable for fatigue limit evaluations, being incapable of calculating finite damage. Papadopoulos' 1994 integral method [15] does not require the definition of load cycles, however, similarly to Dang Van's method, it is only applicable for endurance limit calculations, so it is not able to calculate finite damage. Moreover, Papadopoulos' 2001 further extensions of Dang Van's initial model to finite lives [16] end up requiring the definition of load cycles, or must assume that the loading is periodic. Morel's method [17], on the other hand, does not require the definition of load cycles, since it is based on an integration of the accumulated mesoscopic plastic strain; however, this method is based on strain instead of on fatigue damage integration.

Most works based on the idea of continuous damage evaluation, without cycle detection or counting, use *Continuum Damage Mechanics* (CDM) concepts [18–20]. CDM models describe damage as the progressive loss of material integrity, which supposedly can be inferred from its effect on macroscopic properties such as elastic stiffness or even coefficient of thermal expansion. These global parameters can be a good option for quantifying the deterioration of composites or other materials that fail due to distributed damage. However, for materials that fail by fatigue due to localized damage, like most metallic alloys, CDM approaches need to be supplemented by purely phenomenological damage evolution equations that are difficult to calibrate and sometimes even incompatible with classic and well-proven multiaxial fatigue methods based on the sensible critical-plane idea [7]. In fact, most of these empirical CDM equations are based on mathematical tools that do not provide a better insight into the physical phenomenon, only on its effects.

However, CDM is not the only approach that can lead to incremental damage calculations without the need to identify load cycles. A few local-approach techniques have been proposed based on direct or indirect measures of fatigue damage, through the continuous integration of strain energy density, damage parameters, or fatigue damage itself. These incremental damage models can be divided into two main types: the *Energy Integration* (EI) approach, where the strain energy (either plastic or elastic-plastic) or some other energy-based damage parameter (developed to consider e.g. mean or maximum-stress effects) is directly integrated and compared to a critical value; and the *Incremental Fatigue Damage* (IFD) approach, where fatigue damage itself (instead of an indirect damage parameter) is integrated until reaching a suitable critical value, e.g. 1.0 according to Miner's rule. These two approaches are further discussed next.

2. The energy integration (EI) approach

The EI approach integrates the elastoplastic work or some other energy-based damage parameter along the load path. Under low-cycle multiaxial conditions, this is usually obtained by integrating the product between stress and plastic strain increments for all six components, adding them up into a single scalar quantity. To extend such energy-based models to high-cycle fatigue, measures of the elastic work must also be introduced, otherwise under macroscopically linear elastic (LE) conditions the associated zero plastic work would always predict infinite lives.

Moreover, to consider mean/maximum stress effects on fatigue damage, such elastic-plastic (EP) work parameters are usually multiplied by some stress term to define an energy-based damage parameter (instead of just energy). Such a damage parameter is then integrated along any multiaxial load history path, without the need to project stresses or strains onto any candidate planes, to detect load reversions, or to use any rainflow algorithm to identify individual cycles or equivalent ranges.

The EI approach then *supposes* that crack initiation occurs when the computed energy-based integral reaches a critical value that would be a scalar material constant, independent of the number of applied cycles N. This seems a good idea, but unfortunately the critical accumulated EP work associated with crack initiation is a function of N for most materials. Indeed, the wishful N-independence would require that the material's Coffin-Manson elastic b and plastic c exponents are such that $b + c = -1$, a condition that is not verified in most structural alloys, as shown in Table 1 for well-known εN parameter estimates calibrated for hundreds of materials [1].

As a result, any approach following the direct integration of the strain energy or any other energy-based damage parameter most likely requires the identification of individual cycles to evaluate N, a highly undesired feature. Some EI models implicitly normalize the adopted integral to be able to compare it with a unit critical value; however, by embedding the critical value into the normalized energy-based damage parameter, its calibration should also depend on N. In addition, energy parameters are scalar quantities that do not reflect the directional nature of crack initiation under fatigue loads, which must be considered for so-called directional-damage materials, like most metallic alloys, which fail predominantly due to a single dominant crack. For such important materials, energy parameters should be calculated on individual candidate planes, ignoring in each case any EP work component that does not cause fatigue damage on that particular plane, as in Liu's energy-based critical-plane model [21]. But such energy-based models might require as well cycle detection to compute the critical accumulated damage parameter on the critical plane, if indeed this value is a function of N, as usual.

Table 1
Estimates of Coffin-Manson's elastic and plastic exponents, showing that their sum $b + c$ is not close enough to -1 to justify the existence of a critical energy parameter described by a material constant that is completely independent of N or of the stress or strain amplitudes per cycle.

Estimates	b	c	$b + c$
Manson (1965)	−0.12	−0.6	−0.72
Muralidharan–Manson (1988)	−0.09	−0.56	−0.65
Bäumel–Seeger (steels, 1990)	−0.087	−0.58	−0.667
Bäumel–Seeger (Al & Ti, 1990)	−0.095	−0.69	−0.785
Roessle-Fatemi (2000)	−0.09	−0.56	−0.65
Medians (steels, 2001)	−0.09	−0.59	−0.68
Medians (Al, 2001)	−0.11	−0.66	−0.77

However, fatigue damage models based on the EI approach usually assume the critical value of the chosen energy-based integral is independent of N. Probably the most famous EI model is the *EVent Independent Cumulative Damage* (EVICD) method, proposed in 1987 in Ott's thesis [22] and further developed and reviewed in [23,24]. The method is based on a continuous integration of a damage parameter that combines plastic work with the normal stress on the instantaneous maximum shear stress plane or on octahedral planes, known as EVICD-N or EVICD-J1, respectively. The EVICD-N variation is recommended for *directional-damage materials*, where the mean/maximum-stress effect is controlled by the normal stress $\sigma_\perp$ perpendicular to the critical plane. The EVICD-J1 variation adopts the hydrostatic stress σ_h for mean/maximum-stress effects, so it is applicable for the so-called *distributed-damage materials* (which fail due to distributed damage in all directions), especially if their strengths are pressure-sensitive. But the assumption of plastic (instead of EP) strain energy as the main contributor to fatigue damage makes both EVICD variations limited to ductile materials that display measurable plastic deformation, preventing their use in most high-cycle applications where damage can occur under macroscopically elastic cycles. Furthermore, most EVICD implementations adopt Mróz/Garud kinematic hardening models to calculate the resulting multiaxial plastic strains [25,26], from which plastic work is evaluated. However, Mróz/Garud's multi-linear models can predict false ratcheting even in balanced histories, as well as wrongfully predict zero plastic straining in an EP neutral loading [27].

To avoid these major drawbacks, Jiang et al. implemented the EVICD method [28] using non-linear kinematic (NLK) hardening models instead of Mróz/Garud's, providing reasonable predictions both for low and high-cycle fatigue lives (for their materials) between 10^3 and 10^7 cycles. However, they used the NLK model only to compute multiaxial strains from stresses, considering *plastic memory* but not the important *damage memory* effect discussed by Kreiser et al. [29]. Indeed, the current arrangement of hardening surfaces in the NLK model is used to compute both plastic strains and the energy-based damage parameter, so it assumes that plastic memory and damage memory can be stored with the same set of surfaces. In the next section, it will be shown that accurate damage calculations can only be achieved by adopting two separate and independent sets of surfaces: hardening surfaces for plastic strain calculations, and *damage surfaces* to obtain the resulting damage, which can then be used in Miner's (or any other) damage accumulation rule.

Another cycle-independent model following the EI approach was proposed by Jiang [30], which assumes the plastic strain energy on a material plane is the major cause of fatigue damage, similar to the EVICD-N version of the EVICD method. Damage increments are continuously calculated at every load step as a function of plastic strain energy increments, a mean stress term, and a so-called material memory parameter. But, in addition to the previously discussed issues with adopting energy parameters in a formulation without explicit cycle detection, this model requires the use of a memory surface that expands or contracts following empirical evolution equations, requiring an additional material parameter to control their rate. Moreover, this memory surface works as an indirect way to detect load reversals, which can work for simple multiaxial NP load paths, but probably not for general VAL conditions, which would require several memory surfaces to properly store plastic memory.

Still another EI model was introduced by Kreiser et al. [29], called *Non-Linear Damage Accumulation* (NLDA). The NLDA is based on Ellyin's model [31], which assumes as well that fatigue damage is controlled by the strain energy density. Even though it considers not only plastic but also elastic strain energy, the accumulated total work required to initiate a microcrack is not a material constant and still depends on the number of cycles N, as discussed before; thus it is impossible to calculate without cycle and reversal detection, as desired in a truly cycle-independent fatigue model.

In summary, although EI models can be an interesting energy-based approach to predict fatigue crack initiation, their fitting parameters should be a function of the unknown fatigue life N, still requiring the definition and identification of load cycles; otherwise, their robustness could be compromised if their life predictions are based on model parameters calibrated for a significantly different fatigue life. Nevertheless, if properly calibrated, such energy methods could provide reasonable fatigue life estimates for both constant and variable amplitude loading, as experimentally verified in [32].

3. The incremental fatigue damage (IFD) approach

Instead of integrating strain energy or other energy-based damage parameters, the IFD approach integrates fatigue damage itself. As a result, it follows an idea similar to Miner's rule, integrating differentials of fatigue damage until reaching 1.0 (or any other suitable critical value D_C). No cycle detection or counting is required, since damage is continuously integrated as the loading is applied. For uniaxial histories, this approach makes use of the derivative of the normal stress σ with respect to damage D, called here *generalized damage modulus* D_σ, thus

$$D_\sigma \equiv d\sigma/dD \Rightarrow D = \int dD = \int (1/D_\sigma)\cdot d\sigma \tag{1}$$

For instance, consider a simple uniaxial constant amplitude loading (CAL) history with stress amplitude σ_a. During a load event or half-cycle, the excursion of the stress σ from $-\sigma_a$ to $+\sigma_a$ could be integrated according to Eq. (1) to find the associated fatigue damage $D = 1/2N$, however without explicitly calculating the fatigue life N. The damage D from this half-cycle is initially zero in the load valley when $\sigma = -\sigma_a$, as well as in the beginning the range $\Delta\sigma = \sigma-(-\sigma_a) = 0$, and continuously grows toward the value $D = 1/2N$ until σ reaches the peak $+\sigma_a$, when $\Delta\sigma = \sigma-(-\sigma_a) = 2\sigma a$. To illustrate this idea, Wöhler's stress-based damage model can be adopted for simplicity without considering mean or maximum-stress effects (but these effects, as well as strain-based models, will be discussed later). A simplified relation between the current stress state σ and the continuous damage D from the half-cycle excursion $-\sigma_a \to +\sigma_a$ can then be obtained from Wöhler's curve written in Basquin's notation:

$$\sigma_a = \sigma_c\cdot(2N)^b \Rightarrow \frac{\Delta\sigma}{2} = \frac{\sigma-(-\sigma_a)}{2} = \frac{\sigma_c}{D^b} \Rightarrow D = \left(\frac{\sigma+\sigma_a}{2\sigma_c}\right)^{-1/b} \tag{2}$$

The generalized damage modulus D_σ during this half-cycle is such that

$$\frac{1}{D_\sigma} = \frac{dD}{d\sigma} = -\frac{1}{b(\sigma+\sigma_a)}\left(\frac{\sigma+\sigma_a}{2\sigma_c}\right)^{-1/b} \tag{3}$$

from which the fatigue damage $D = 1/2N$ can be calculated using the integral

$$D = \int_{-\sigma_a}^{+\sigma_a} -\frac{1}{b(\sigma+\sigma_a)}\left(\frac{\sigma+\sigma_a}{2\sigma_c}\right)^{-1/b}\cdot d\sigma = \left(\frac{\sigma+\sigma_a}{2\sigma_c}\right)^{-1/b}\Bigg|_{-\sigma_a}^{+\sigma_a} = \left(\frac{\sigma_a}{\sigma_c}\right)^{-1/b} = \frac{1}{2N} \tag{4}$$

If this conceptually simple procedure could be generalized to multiaxial NP VAL histories, integrating damage along a general multiaxial load path, then cycle identification, multiaxial rainflow counting, and stress (or strain) range calculations would not be required to obtain the resulting fatigue damage D. However, this nice statement is easier said than done, since D_σ depends not only on the current stress state (σ in this uniaxial case), but also on the previous loading history (the value $-\sigma_a$ from the last reversal), see Eq. (3). So, IFD models need to allow D_σ to vary as a function of the stress level and of the existing state of damage [27], a challenging task for multiaxial NP histories.

3.1. Early incremental fatigue damage models

Wetzel and Topper proposed in 1971 the first uniaxial incremental fatigue model [33]. This pioneer IFD model predicts fatigue crack initiation associating damage with discretized elements of a uniaxial stress-strain model. Plastic memory is stored using Martin-Topper-Sinclair's rheological model and push-stack algorithm [34,35], which automatically reproduces Masing's behavior and the rainflow method under uniaxial conditions [1]. Wetzel used each element of the stress-strain model not only to evaluate plastic strains, but also fatigue damage, storing in this way the *damage memory* required for a correct damage integration in cyclic histories. Even though the push-stack concept is able to detect and count cycles in uniaxial histories, fatigue damage integration is continuously carried out without waiting for each hysteresis loop to close, thus Wetzel's work can indeed be classified as a truly IFD approach method, albeit limited to uniaxial loads. Landgraf et al. [36] discussed in 1975 the implementation of Wetzel's method in fatigue life predictions for notched members under VAL. However, they ended up following the traditional discrete path consisting of damage calculation for closed hysteresis loops, instead of using a continuous numeric integration of fatigue damage along the (uniaxial) load path.

It was only in 2000 that Wetzel's idea was finally revisited, in Chu's IFD method [37]. Chu multiplied the calculated fatigue damage differentials by a stress term similar to Goodman's, thus including mean/maximum-stress effects in Wetzel's uniaxial IFD model. Moreover, Chu outlined the generalization of Wetzel's model to multiaxial NP loadings, indirectly detecting cycles using two simple rules for tracking the so-called damage rate (the inverse of the previously defined generalized damage modulus D_σ) with respect to the stress amplitude. This alternative definition of closed hysteresis loops is used for multiaxial fatigue histories based on an equivalent von Mises stress, to reduce the problem to a uniaxial one. This approach is appropriate for multiaxial *proportional* loadings, but the damage memory is not properly stored for NP VAL histories, where often no hysteresis loop actually closes, so any virtual loop closure detection makes no sense. Chu's IFD model still depends on the definition of a load reversal for NP histories, because no proper internal material variables were defined to store the existing state of damage, which affects D_σ according to [29], as discussed before.

Moreover, Chu performs fatigue damage integration using von Mises stresses both in the damage parameter and in the load reversal criterion, without projecting the original stresses onto suitable candidate planes. Therefore, Chu's method mixes damage on different material planes, certainly not a recommended practice for so-called directional-damage materials like most metallic alloys, which usually initiate a single dominant fatigue crack.

Besides Wetzel's method (improved by Chu), another major IFD model is the *Integration of Damage Differentials* (IDD), proposed in 1993 by Stefanov [38–43]. He defined a so-called curvilinear integral based on the idea of damage integration, restricted for high-cycle fatigue. Despite a good agreement with some experimental data, his method requires heuristic case-by-case calibration of damage derivatives with respect to normal or shear stresses, called damage intensities or R-functions (which, for the normal stress component, is the inverse of the parameter D_σ defined above). Such R-functions for shear histories or NP loading are frequently assumed equal to uniaxial values, and empirically combined using a simple Euclidean norm. Perhaps the need for specialized software to solve the complex elliptic equations, as well as the complexity involved in an accurate R-function calibration, has prevented the widespread use of the IDD method.

Another issue with the IDD is that it neglects the damage dependence on the load history (the damage memory), because there are no internal variables to store the current material state. Therefore, the R-functions calibrated for simple loading histories might not reproduce the damage evolution induced by a complex NP multiaxial history.

In addition, the IDD method mixes damage from different planes, caused e.g. by orthogonal normal stress histories $\sigma_x(t)$ and $\sigma_y(t)$. This does not agree with the critical-plane approach preferred for directional-damage materials like most metallic alloys, since a single dominant microcrack initiating on a plane perpendicular to $\sigma_x(t)$ should not be influenced by the $\sigma_y(t)$ history, and vice versa. Therefore, their damage contributions should not be combined, unless the microcrack plane keeps changing, or the material fails due to distributed damage in several directions. It could be argued that a case where all material planes suffer the same critical damage should result in a lower fatigue life than a case where only one plane suffers this very same damage [44]; however, if it fails due to a single dominant microcrack, this difference should not be large enough to justify the direct mixture of damage planes, instead of following a critical-plane approach.

In the next section, the general IFD approach proposed in this work is detailed.

4. Incremental fatigue with damage surfaces

The history-dependence of the generalized damage modulus D_σ is analogous to the load-order dependence of EP hysteresis loops, but this damage memory is often neglected or overly simplified in the few IFD models available. For instance, Wetzel's model accounts for both plasticity and damage memory, using the rheological model from Fig. 1. For plasticity calculations, its spring stiffnesses H_i from Fig. 1 are calibrated from the stress-strain curve, while for damage computations they are calibrated from the adopted damage equation. However, Wetzel's rheological model for damage calculation is only applicable for uniaxial histories, and it does not include mean/maximum-stress effects.

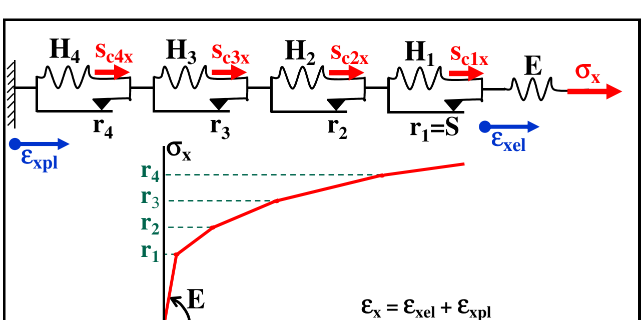

Fig. 1. Uniaxial rheological model for kinematic hardening with a series of spring-slider elements of stiffness H_i and slider threshold r_i, and resulting stress-strain curve under monotonic tension.

Alternatively to rheological models, a direct analogy between IFD and incremental plasticity could be used to store damage memory using internal material variables. In incremental plasticity, a 5D deviatoric stress increment $d\vec{s}'$ can be used to calculate the associated 5D plastic strain increment $d\vec{e}'_{pl}$ from the current generalized plastic modulus P, using a plastic flow rule [1,45]. In the NLK incremental plasticity formulation, *plastic memory* is stored by the current arrangement among the hardening surfaces defined by their backstresses $\vec{\beta}'_i$, from which the *surface translation directions* $\vec{v}'_i$ are calculated (according to some translation rule) and combined with p_i coefficients to calculate the current P. No *plastic straining* occurs if the stress increment $d\vec{s}'$ happens inside the *yield surface*, whose radius should be equal or smaller than the *cyclic yield strength* S_{Yc}. The *accumulated plastic strain* p is then proportional to the integral of the scalar norm $|d\vec{e}'_{pl}|$ of the deviatoric plastic strain increments.

Let's now describe the proposed multiaxial IFD model using a direct plasticity-damage analogy. In it, a 5D deviatoric stress increment $d\vec{s}'$ can be used to calculate the associated 5D *damage* increment $d\vec{D}'$ from the current *generalized damage modulus* D_σ, using a *damage evolution rule*. In the IFD formulation, *damage memory* is stored by the current arrangement among *damage surfaces* defined by their *damage backstresses* $\vec{\beta}'_{\sigma_i}$, from which the *damage surface translation directions* $\vec{v}'_{\sigma_i}$ are calculated (according to some translation rule) and combined with $d_{\sigma i}$ coefficients to calculate the current D_σ. No *damage* occurs if the stress increment $d\vec{s}'$ happens inside the *fatigue limit surface*, whose radius should be equal or smaller than the *fatigue limit* S_L. The *accumulated damage* D is then equal to the integral of the scalar norm $|d\vec{D}'|$ of the damage increments. The damage backstress vector $\vec{\beta}'_\sigma$ locates the center of the current fatigue limit surface, which can be decomposed as the sum of M damage backstresses $\vec{\beta}'_{\sigma_1}, \vec{\beta}'_{\sigma_2}, \ldots, \vec{\beta}'_{\sigma_M}$ that describe the relative positions between centers of M consecutive damage surfaces, as illustrated in Fig. 2 for a 2D case. Note that the radius of the fatigue limit surface can be set very close to zero if the material does not have a clear fatigue limit.

Each damage surface has a *constant* radius $r_{\sigma i}$, while the radius differences between consecutive surfaces are defined as $\Delta r_{\sigma i} = r_{\sigma i+1} - r_{\sigma i}$. The fatigue limit surface and the failure surface are defined, respectively, for $i = 1$ and $i = M + 1$, while the remaining $i = 2, 3, \ldots, M$ are the damage surfaces. The lengths (norms) $|\vec{\beta}'_{\sigma_i}|$ are always between $|\vec{\beta}'_{\sigma_i}| = 0$, if consecutive centers coincide, and $|\vec{\beta}'_i| = \Delta r_{\sigma_i}$, if the damage surfaces are mutually tangent.

If a Mróz multi-surface formulation [25] was used for this IFD model, then the radii $r_{\sigma i}$ of the various damage surfaces would be equal to the stress levels associated with the chosen damage values $D_{\sigma i}$ that delineate the multi-linear representation of the damage curve, see Fig. 3. Moreover, the slopes of this piecewise linearization would be the generalized damage moduli $D_{\sigma i}$, for $i = 1, 2, \ldots, M + 1$. The calibration of these $D_{\sigma i}$ could adopt, e.g., Basquin's representation of Wöhler's curve to correlate stress and damage, see Eq. (3).

However, the Mróz multi-surface formulation has several issues [27]. For incremental plasticity problems, it can predict false ratcheting even in balanced load histories, as well as wrongfully predict zero plastic straining in EP neutral loadings. Analogously, if used in the IFD context, such a formulation could predict an increase or decrease in damage per cycle even for multiaxial constant amplitude loadings, as well as wrongfully predict zero damage for a circular loading history following the contour of a damage surface (which is always larger than the fatigue limit surface and thus should result in damage). Wetzel's damage calculation approach using the rheological model from Fig. 1 would exactly reproduce the Mróz multi-surface formulation, thus presenting the same issues.

Therefore, even though damage memory is considered here through multiple damage surfaces, a NLK formulation is adopted for the proposed IFD model, allowing *all* surfaces to translate during a damage process (instead of just the active surface and the inner ones, as in the Mróz formulation). So, this non-linear IFD model uses a 5D damage vector $\vec{D}' \equiv [D_1\ D_2\ D_3\ D_4\ D_5]^T$ that acts as an internal variable that stores the current damage state (to account for the damage memory). The scalars D_1 through D_5 are signed damage quantities associated with each one of the 5D deviatoric stress vector $\vec{s}_i'$ directions. The 5D space adopted here represents deviatoric stresses $\vec{s}'$ and deviatoric elastic and plastic strains $\vec{e}_{el}'$ and $\vec{e}_{pl}'$ as

$$\vec{s}' \equiv [s_1\quad s_2\quad s_3\quad s_4\quad s_5]^T,\quad \vec{e}_{el}' \equiv [e_{1_{el}}\quad e_{2_{el}}\quad e_{3_{el}}\quad e_{4_{el}}\quad e_{5_{el}}]^T,$$
$$\vec{e}_{pl}' \equiv [e_{1_{pl}}\quad e_{2_{pl}}\quad e_{3_{pl}}\quad e_{4_{pl}}\quad e_{5_{pl}}]^T \tag{5}$$

where

$$\begin{cases} s_1 \equiv \sigma_x - (\sigma_y + \sigma_z)/2 = 3s_x/2,\ \ s_2 \equiv (\sigma_y - \sigma_z)\sqrt{3}/2 = (s_y - s_z)\sqrt{3}/2 \\ s_3 \equiv \tau_{xy}\sqrt{3},\ \ s_4 \equiv \tau_{xz}\sqrt{3},\ \ s_5 \equiv \tau_{yz}\sqrt{3} \end{cases} \tag{6}$$

$$\begin{cases} e_{1_{el}} \equiv \varepsilon_{x_{el}} - \frac{\varepsilon_{y_{el}}+\varepsilon_{z_{el}}}{2} = \frac{3}{2}e_{x_{el}},\quad e_{2_{el}} \equiv \frac{\varepsilon_{y_{el}}-\varepsilon_{z_{el}}}{2}\sqrt{3} = \frac{e_{y_{el}}-e_{z_{el}}}{2}\sqrt{3} \\ e_{3_{el}} \equiv \frac{\gamma_{xy_{el}}}{2}\sqrt{3},\quad e_{4_{el}} \equiv \frac{\gamma_{xz_{el}}}{2}\sqrt{3},\quad e_{5_{el}} \equiv \frac{\gamma_{yz_{el}}}{2}\sqrt{3} \end{cases} \tag{7}$$

$$\begin{cases} e_{1_{pl}} \equiv \varepsilon_{x_{pl}} - \frac{\varepsilon_{y_{pl}}+\varepsilon_{z_{pl}}}{2} = \frac{3}{2}e_{x_{pl}},\quad e_{2_{pl}} \equiv \frac{\varepsilon_{y_{pl}}-\varepsilon_{z_{pl}}}{2}\sqrt{3} = \frac{e_{y_{pl}}-e_{z_{pl}}}{2}\sqrt{3} \\ e_{3_{pl}} \equiv \frac{\gamma_{xy_{pl}}}{2}\sqrt{3},\quad e_{4_{pl}} \equiv \frac{\gamma_{xz_{pl}}}{2}\sqrt{3},\quad e_{5_{pl}} \equiv \frac{\gamma_{yz_{pl}}}{2}\sqrt{3} \end{cases} \tag{8}$$

The accumulated damage D (analogous to the accumulated plastic strain p) is obtained from the length of the path described by the 5D damage vector $\vec{D}'$, calculated in either continuous or discrete formulations from

$$D = \int_{path} dD = \int_{path} |d\vec{D}'| \cong \sum_{path} \Delta D = \sum_{path} |\Delta\vec{D}'| \tag{9}$$

If a given deviatoric stress state $\vec{s}'$ is on the fatigue limit surface with a normal unit vector $\vec{n}_\sigma'$, and if its infinitesimal increment $d\vec{s}'$ is in the outward direction, then $d\vec{s}'^T \cdot \vec{n}_\sigma' > 0$ and a fatigue damage increment is obtained from a *damage evolution rule* (inspired on the Prandtl-Reuss flow rule):

$$d\vec{D}' = (1/D_\sigma) \cdot (d\vec{s}'^T \cdot \vec{n}_\sigma') \cdot \vec{n}_\sigma' \cdot f_{MS}(\vec{\sigma}) \tag{10}$$

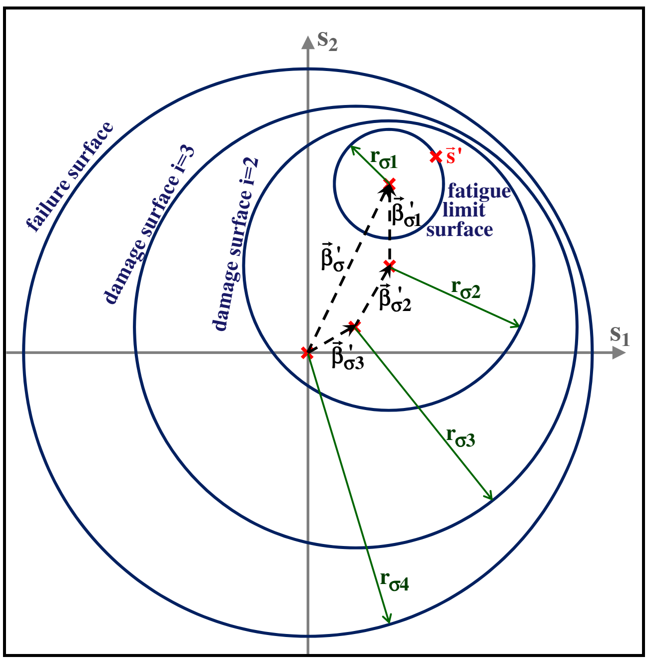

Fig. 2. Fatigue limit, damage, and failure surfaces in the deviatoric stress space for $M = 3$, showing the damage backstress vector $\vec{\beta}_\sigma'$ that defines the location of the fatigue limit surface center, and its components $\vec{\beta}_{\sigma_1}'$, $\vec{\beta}_{\sigma_2}'$, and $\vec{\beta}_{\sigma_3}'$ that describe the relative positions between the centers of the M consecutive damage surfaces.

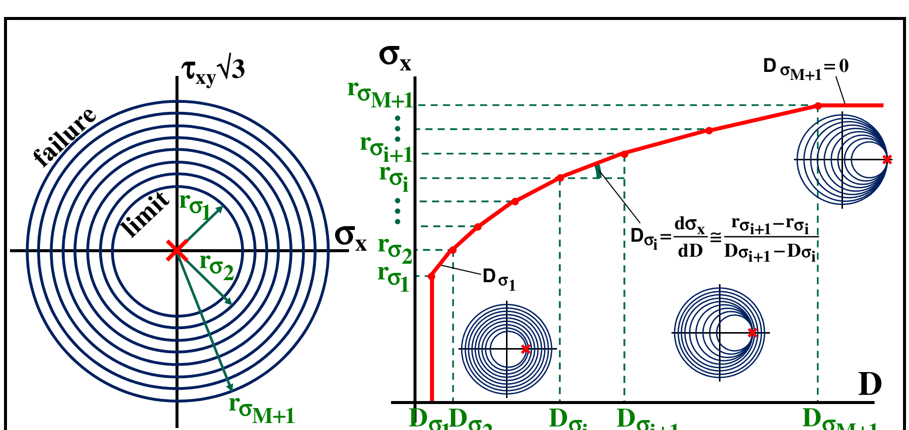

Fig. 3. Fatigue limit, damage, and failure surfaces in the $\sigma_x \times \tau_{xy}\sqrt{3}$ 2D sub-space of the deviatoric stress space, and corresponding radii $r_{\sigma i}$ and generalized damage moduli $D_{\sigma i}$ obtained from the piecewise linearization of the uniaxial stress × damage curve (right). Stress amplitudes below $r_{\sigma 1}$ are assumed to cause no damage, thus the vertical slope at $D_{\sigma 1}$.

where $f_{MS}(\vec{\sigma})$ is a scalar *mean stress function* of the current 6D stress $\vec{\sigma}$ to account for mean or maximum-stress effects, which can be defined e.g. from Goodman's or Gerber's (σ_a; σ_m) relations. For distributed-damage materials, the mean stress function $f_{MS}(\vec{\sigma})$ could be based on the current hydrostatic stress σ_h, while for directional-damage materials (which require the critical-plane approach) $f_{MS}(\vec{\sigma})$ could be based on the normal stress $\sigma_\perp$ perpendicular to the candidate plane.

It is important to note that fatigue damage is not a proper physical quantity, at least when defined as a non-dimensional value between 0 and 1. Therefore, Eq. (10) cannot be a physical law, since it is intrinsically empirical in nature. Nevertheless, it has a mathematical foundation: it quantifies variations within a potential field, in this case the damage field defined by the adopted nested surfaces. Since variations within any potential field must be computed normal to iso-potential surfaces, it is easy to justify why the damage increments from Eq. (10) are calculated in the direction $\vec{n}'_\sigma$ normal to the damage surfaces. In the same way that empirical fatigue damage models have been successfully used in engineering practice, empirical evolution rules such as Eq. (10) can be much useful in practice. In addition, the proposed IFD model can be easily calibrated from traditional $SN/\varepsilon N$ curve equations, as opposed to CDM models that need purely mathematical damage evolution equations that are difficult to calibrate and usually are not related to classic and well-proven fatigue models.

Except for the failure surface (which never translates), during this damage process the fatigue limit and all damage surfaces suffer translations given by

$$d\vec{\beta}'_{\sigma i} = \begin{cases} d_{\sigma i} \cdot \vec{v}'_{\sigma i} \cdot dD, & if |\vec{\beta}'_{\sigma i}| < \Delta r_{\sigma i} \\ 0, & if |\vec{\beta}'_{\sigma i}| = \Delta r_{\sigma i} \end{cases} \tag{11}$$

where $d_{\sigma i}$ are coefficients calibrated for each surface, and $\vec{v}'_{\sigma_i}$ are the *damage surface translation directions* adapted e.g. from the general translation rule from [25]. For instance, Jiang-Sehitoglu's translation rule [46] gives the adapted expression

$$\vec{v}'_{\sigma i} = \vec{n}'_\sigma \cdot \Delta r_{\sigma i} - \left(|\vec{\beta}'_{\sigma i}| \big/ \Delta r_{\sigma i}\right)^{\chi_{\sigma i}} \cdot \vec{\beta}'_{\sigma i} \tag{12}$$

where $\chi_{\sigma i}$ are fitting exponents for each damage surface.

The current generalized damage modulus D_σ is then obtained from the consistency condition, which guarantees that the current stress state is never outside the fatigue limit surface, taken from an analogy to the NLK formulation

$$D_\sigma = \left(\sum_{i=1}^{M} d_{\sigma i} \cdot \vec{v}'^{T}_{\sigma i}\right) \cdot \vec{n}'_\sigma \tag{13}$$

allowing the calculation of the evolution of the damage vector $\vec{D}'$ from Eq. (10).

The (scalar) accumulated damage D is then obtained from Eq. (9). This formulation can deal with any multiaxial stress history, proportional or NP, and eliminates the need to define or count cycles and find equivalent ranges, the major advantage of the proposed IFD model.

To exemplify these ideas, Fig. 4 shows IFD predictions for a material with Basquin's parameters $\sigma_c = 772.5$ MPa and $b = -0.09$, under the uniaxial loading history $\sigma_x = \{0 \to 300 \to -300 \to 300\}$ MPa. Jiang-Sehitoglu's translation rule was adopted with $M = 16$ surfaces, $D_{\sigma 1} = 10^{-8}$ (or any other small threshold value for the fatigue limit), and $D_{\sigma M+1} = 0.01$ (to improve the calculation accuracy and reduce the computational cost as opposed to Miner's $D_{\sigma M+1} = 1.0$, appropriate as long as no single half-cycle from the history is able to cause a damage increment greater than 0.01). The above calibration routine was applied using exponents $\chi_{\sigma i} = 100$ ($i = 1, \ldots, 16$), an arbitrary high value that does not affect the predictions.

Fig. 4 (left) shows the hysteresis loops $\sigma_x \times D_1$, where D_1 is the first component of the previously defined 5D damage vector $\vec{D}'$. Notice in this figure that damage components such as D_1 can become negative, as a result of an unloading process. This is not an issue, since $\vec{D}'$ is just an internal variable used to calculate the actual fatigue damage. Indeed, the accumulated damage D is obtained from the integral of the norm of the infinitesimal increments $|d\vec{D}'|$, see Eq. (9). It is important to emphasize that this elementary loading example is linear elastic, without any significant macroscopic plasticity; the non-linear shape of the stress × damage hysteresis loops is just a consequence of the non-linearity of Wöhler-Basquin's damage equation.

Fig. 4 (right) shows the resulting accumulated damage D as a function of an accumulated stress, defined as the integral of the infinitesimal deviatoric increments' norm $|d\vec{s}'|$ (which is analogous to the accumulated plastic strain p, but defined for stresses). The depicted *theoretical* (discrete) *damage* is calculated in the

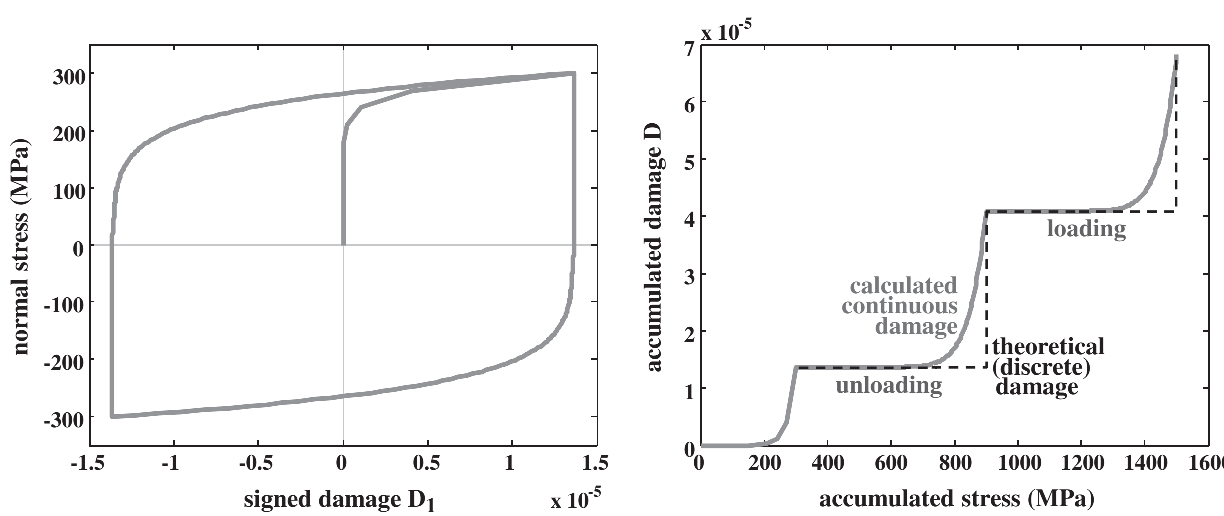

Fig. 4. Stress × damage hysteresis loops for a uniaxial history (left), and resulting accumulated damage as a function of accumulated stress (right).

traditional way after counting each one of the three rainflow half-cycles {0 → 300}, {300 → −300} and {−300 → 300} MPa. Notice how the continuous IFD calculations almost exactly reproduce, at the end of each half-cycle, the discrete predictions. But in IFD the calculated damage is continuous and does not require rainflow counts, or even the definition or detection of a half-cycle.

One small issue with the non-linear IFD approach is the fact that it assumes the damage from the initial event {0 → 300} as exactly half of the damage from {−300 → 300} MPa, when in fact it should be much smaller due to non-linearity in the damage equation. This is because the IFD model implicitly assumes that another event {−300 → 0} will happen in the future, which would be combined with the previous {0 → 300} to correctly add both damage halves into 1.0. This issue is irrelevant, since it will only affect the stress path along the inner curve in Fig. 4 (left), which ends up contributing only as a single half-cycle, no matter how long the history is. However, for a clearer comparison of the subsequent events, the theoretical damage calculation in Fig. 4 (right) exceptionally adopted the IFD's half-damage value for the initial event.

Note that this trivial uniaxial example ignored mean/maximum-stress effects, adopting a mean stress function $f_{MS}(\vec{\sigma}) \equiv 1$. Future works will address the inclusion of such effects, e.g. using mean stress functions inspired on Fatemi-Socie's damage parameter.

The presented non-linear IFD approach is not really needed to analyze uniaxial load histories, where cycle detection is simple and the (uniaxial) rainflow method is sufficient to count them. The main advantage of this approach is for multiaxial histories, where cycle detection and counting are still open problems that depend on the adopted damage calculation routine.

For distributed-damage materials, invariant-based damage models could be calibrated using the non-linear IFD approach with the presented 5D definition of the damage vector $\vec{D}'$. For directional-damage materials, which require the critical-plane approach [7], the same non-linear IFD model could be adopted, but only for the projected components on the studied candidate plane. For instance, for a shear-based multiaxial damage model, a 2D damage vector $\vec{D}'$ could be correlated with the $[\tau_A \ \tau_B]$ sub-space of the candidate plane shear stresses.

All the formulations and the example presented above assumed nominally linear elastic loading histories at the macroscopic scale, whose damage can be calculated from *SN* models such as Wöhler-Basquin's and Goodman, but this is not a limitation for this methodology. Indeed, the proposed IFD approach can be as well extended for EP loading histories, whose fatigue damage must be quantified by εN models. However, instead of using fatigue limit and damage surfaces defined in stress spaces, strain spaces should be used in the continuous damage calculations in such cases. A generalized damage modulus D_ε (instead of D_σ) is thus defined, which for uniaxial loading histories becomes the derivative of the normal strain ε with respect to damage D, thus $D_\varepsilon \equiv d\varepsilon/dD$.

In the strain-based version of the proposed IFD approach, the 5D deviatoric strain increment $d\vec{e}'$, defined in the 5D deviatoric strain spaces from Eqs. (5)–(8), is used to calculate the associated 5D *damage* increment $d\vec{D}'$ from the current D_ε, using a suitable *damage evolution rule*. To do so, *damage memory* is stored by the current arrangement among *damage surfaces* defined by their *damage backstrains* $\vec{\beta}'_{\varepsilon i}$, from which the *damage surface translation directions* $\vec{v}'_{\varepsilon i}$ are calculated according to some translation rule and combined with material coefficients $d_{\varepsilon i}$ to calculate the current D_ε. The *accumulated damage D* is then equal to the integral of the scalar norm $|d\vec{D}'|$ of the damage increments. The same equations from the stress-based version can be used in the strain-based one, as long as the *M* damage surface backstrains $\vec{\beta}'_{\varepsilon 1}$, $\vec{\beta}'_{\varepsilon 2}$, …, $\vec{\beta}'_{\varepsilon M}$, radii $r_{\varepsilon i}$, and radius differences $\Delta r_{\varepsilon i} \equiv r_{\varepsilon i+1} - r_{\varepsilon i}$ between consecutive damage surfaces are all defined as strain (instead of stress) quantities.

5. Experimental results

The proposed IFD formulation is experimentally evaluated using complex 2D tension-torsion stress histories, applied on annealed tubular 316L stainless steel specimens in a tension-torsion servo-hydraulic testing machine, see Fig. 5. The Coffin-Manson curve for this material is

$$\Delta\varepsilon/2 = 0.0119 \cdot (2N)^{-0.277} + 0.758 \cdot (2N)^{-0.582} \tag{14}$$

obtained from uniaxial εN tests.

The experiments consist of strain-controlled tension-torsion cycles applied to eight tubular specimens, each one of them following one of the eight periodic $\varepsilon_x \times \gamma_{xy}/\sqrt{3}$ histories from Fig. 6. All the tests were carried out until a small crack was detected on the surface by visual inspection. In all specimens, the initiated crack was later confirmed to have surface widths between 1 and 2 mm. This variability contributes to the uncertainties in the experimental data, even though it can be inferred that the number of growth cycles between 1 and 2 mm should be relatively small, since the visual inspection was carried out on a frequent basis.

Table 2 compares the predicted and observed fatigue lives in number of blocks, where each block consists of a full load period. All predictions were performed using the strain-based version of the proposed incremental plasticity formulation, assuming for simplicity $f_{MS}(\vec{\sigma}) \equiv 1$ in Eq. (10).

As shown in Table 2, albeit the proposed IFD method does not use any cycle detection or counting algorithm, all fatigue lives are predicted with relatively small errors, well within the usual scatter found in all fatigue life measurements. It also automatically applies Miner's rule under VAL, as it can be seen in the loading path consisting of blocks of consecutive square and cross paths, since the predicted number of blocks 482 is such that $1/482 \cong 1/751 + 1/1314$.

Similarly, the predicted 327 blocks of consecutive square, circle and diamond paths is such that $1/327 \cong 1/751 + 1/996 + 1/1436$. Miner's rule was also confirmed within the observed experimental results, since e.g. in this latter case it would predict a life of $1/(1/772 + 1/837 + 1/976) = 285$ blocks, almost the same value as the measured 288 blocks. Note that all the predictions listed in Table 2 were based only on uniaxial Coffin-Manson data, without any posterior curve fitting procedure.

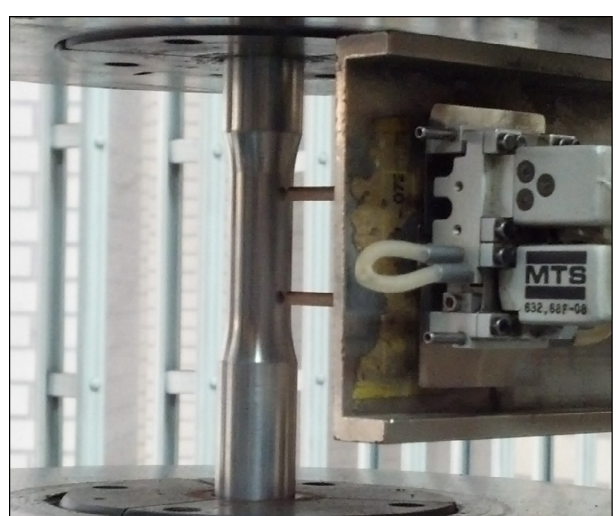

Fig. 5. Tubular specimen mounted in a tension-torsion fatigue testing machine, showing the axial/torsional extensometer.

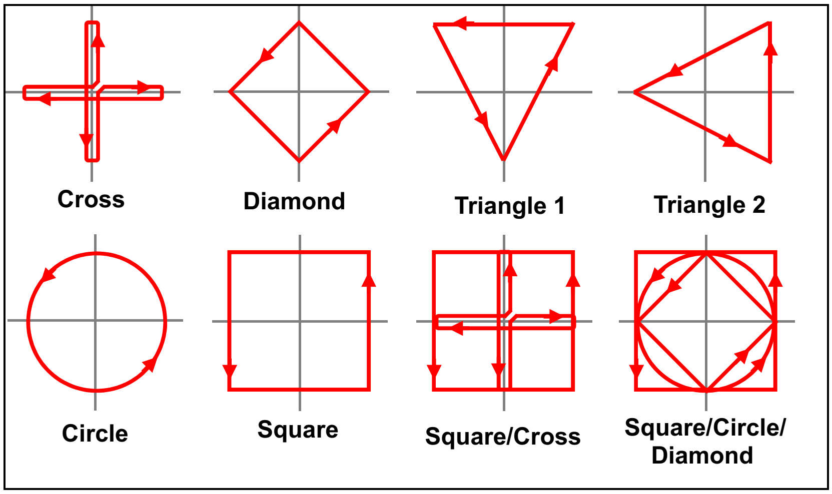

Fig. 6. Applied periodic $\varepsilon_x \times \gamma_{xy}/\sqrt{3}$ strain paths on eight tension-torsion tubular specimens, all of them with normal and effective shear amplitudes 0.6%.

Table 2
Predicted and observed lives, in number of blocks, for each applied path.

Tension-torsion path	Predicted	Observed	Error (%)
Cross	1314	1535	−14
Diamond	1436	976	+47
Triangle 1	1135	842	+35
Triangle 2	1180	840	+40
Circle	996	837	+19
Square	751	772	−3
Square/Cross	482	342	+41
Square/circle/diamond	327	288	+14

As discussed above, the proposed method automatically reproduces Miner's rule because of Eq. (9), which states that the resulting fatigue damage is a result of the integral over the path, therefore it would be linearly additive. Miner's rule still is the best engineering tool for both high and low-cycle fatigue, however under low-cycle conditions the order of the loading must be considered, to properly account for residual stress effects and plastic memory in general. However, such effects are intrinsically considered in the proposed approach, since any stress-strain calculations should be performed before fatigue damage integration, in a separate incremental plasticity framework that considers the load order. Therefore, all non-linearities and load order effects due to plasticity are already considered in the proposed IFD model.

Nevertheless, it is important to note that Miner's rule is not a physical law. Therefore it can still result in significant prediction errors for some particularly ordered histories, or in variable amplitude histories with large variations in stress or strain amplitude. In fact, the square/circle/diamond and the square/cross paths probably resulted in such an unusually high experimental agreement with Miner's rule because they involved similar (although not equal) path-equivalent strain amplitudes.

6. Conclusions

A continuous multiaxial Incremental Fatigue Damage formulation is proposed in this work, based on a direct analogy with incremental plasticity models. Both proposed stress and strain-based approaches can be formulated using traditional stress, strain, or even energy-based *SN* and εN damage models, such as Wöhler-Basquin, Coffin-Manson, Smith-Watson-Topper, or Fatemi-Socie, making it an attractive and practical tool for engineering use. In particular, the proposed IFD models do not require additional fitting parameters, or complex calibration routines, as opposed to equally continuous models that are based on traditional Continuum Damage Mechanics approaches. The experimental results show that the proposed method is able to predict quite well multiaxial fatigue lives under complex tension-torsion histories, even though it does not require any cycle detection, multiaxial rainflow counting, or path-equivalent range computations.

Acknowledgments

This work was supported in part by the National Natural Science Foundation of P.R. China under Grant No. 11302150. CNPq-Brazil provided a fellowship for Prof. Marco A. Meggiolaro.

References

[1] Castro JTP, Meggiolaro MA. Fatigue design techniques: Vol. II – low-cycle and multiaxial fatigue. Scotts Valley (CA) USA: CreateSpace Publishing Company; 2016.
[2] Langlais TE, Vogel JH, Chase TR. Multiaxial cycle counting for critical plane methods. Int J Fatigue 2003;25:641–7.
[3] Meggiolaro MA, Castro JTP, Wu H. Invariant-based and critical-plane rainflow approaches for fatigue life prediction under multiaxial variable amplitude loading. Proc Eng 2015;101:69–76.
[4] Wang CH, Brown MW. Life prediction techniques for variable amplitude multiaxial fatigue – Part 1: Theories. J Eng Mater Technol 1996;118:367–70.
[5] Meggiolaro MA, Castro JTP. An improved multiaxial rainflow algorithm for non-proportional stress or strain histories – Part II: The modified Wang-Brown method. Int J Fatigue 2012;42:194–206.
[6] Dong P, Wei Z, Hong JK. A path-dependent cycle counting method for variable amplitude multiaxial loading. Int J Fatigue 2010;32:720–34.
[7] Bannantine JA, Socie DF. A variable amplitude multiaxial fatigue life prediction method. In: Fatigue under biaxial and multiaxial loading. ESIS Publication 10:35-51; 1991.
[8] Carpinteri Andrea, Spagnoli Andrea, Ronchei Camilla, Scorza Daniela, Vantadori Sabrina. Critical plane criterion for fatigue life calculation: time and frequency domain formulations. Proc Eng 2015;101:518–23.
[9] Meggiolaro MA, Castro JTP. An improved multiaxial rainflow algorithm for nonproportional stress or strain histories – Part I: Enclosing surface methods. Int J Fatigue 2012;42:217–26.
[10] Majumdar S, Maiya PS. A mechanistic model for time-dependent fatigue. J Eng Mater Technol 1980;111:123–31.
[11] Murakami S. Progress of continuum damage mechanics. JSME Int J A – Solid Mech Mater Eng 1987;30:701–10.
[12] Lemaitre J, Plumtree A. Application of damage concept to predict creep-fatigue failure. J Eng Mater Technol 1979;101:284–92.
[13] Tinga T, Brekelmans WAM, Geers MGD. Time-incremental creep–fatigue damage rule for single crystal Ni-base superalloys. Mater Sci Eng A 2009;508:200–8.
[14] Dang Van K, Griveau B, Message O. On a new multiaxial fatigue limit criterion: theory and application. Biaxial and multiaxial fatigue, EFG Publication 3:479-496; 1989.

[15] Papadopoulos IV. A new criterion of fatigue strength for out-of-phase bending and torsion of hard metals. Int J Fatigue 1994;16(6):377–84.
[16] Papadopoulos IV. Long life fatigue under multiaxial loading. Int J Fatigue 2001;23:839–49.
[17] Morel F. A critical plane approach for life prediction of high cycle fatigue under multiaxial variable amplitude loading. Int J Fatigue 2000;22:101–19.
[18] Krajcinovic D. Damage Mechanics. Amsterdam; 1996.
[19] Murakami S. Continuum damage mechanics: a continuum mechanics approach to the analysis of damage and fracture. Springer; 2012.
[20] Armero F, Oller S. A general framework for continuum damage models I – infinitesimal plastic damage models in stress space. Int J Solids Struct 2000;37:7409–36.
[21] Liu KC. A method based on virtual strain-energy parameters for multiaxial fatigue life prediction. ASTM STP 1993;1191:67–84.
[22] Ott W. Neues Verfahren zur Betriebsfestigkeitsanalyse komplexer Bauteile auf der Grundlage der FEM Ph.D. Thesis. Germany: U Aachen (RWTH); 1987.
[23] Ott W, Baumgart O, Trautmann KH, Nowack H. A new crack initiation life prediction method for arbitrary multiaxial loading considering mean stress effect. In: P 6th Int Fatigue Conf (FATIGUE'96), Germany. p. 1007–12.
[24] Nowack H, Baum C, Ott W, Buczynski A, Glinka G. Achievements of the incremental multiaxial fatigue prediction method EVICD. In: P 5th Int Conf Low Cycle Fatigue, Germany. p. 277–82.
[25] Mróz Z. On the description of anisotropic workhardening. J Mech Phys Solids 1967;15:163–75.
[26] Garud YS. A new approach to the evaluation of fatigue under multiaxial loading. J Eng Mater Technol 1981;103:118–25.
[27] Meggiolaro MA, Castro JTP, Wu H. A general class of non-linear kinematic models to predict mean stress relaxation and multiaxial ratcheting in fatigue problems – Part II: Generalized yield surface translation rule. Int J Fatigue 2016;82:167–78.
[28] Jiang Y, Ott W, Baum C, Vormwald M, Nowack H. Fatigue life predictions by integrating EVICD fatigue damage model and an advanced cyclic plasticity theory. Int J Plasticity 2009;25:780–801.
[29] Kreiser D, Jia SX, Han JJ, Dhanasekar M. A nonlinear damage accumulation model for shakedown failure. Int J Fatigue 2007;29:1523–30.
[30] Jiang Y. A fatigue criterion for general multiaxial loading. Fatigue Fract Eng Mater Struct 2000;23:19–32.
[31] Ellyin F, Golos K. A total strain energy density theory for cumulative fatigue damage. J Press Vess Technol 1998;110:36–41.
[32] Saintier N, Palin-Luc T, Bénabès J, Cocheteux F. Non-local energy based fatigue life calculation method under multiaxial variable amplitude loadings. Int J Fatigue 2013;54:68–83.
[33] Wetzel RM. A method of fatigue damage analysis Ph.D. Thesis. U Waterloo; 1971.
[34] Martin JF, Topper TH, Sinclair GM. Computer based simulation of cyclic stress-strain behavior with applications to fatigue. Mater Res Standards 1971;11:23–9.
[35] Conle FA. A computer simulation assisted statistical approach to the problem of random fatigue M.Sc Thesis. University of Waterloo; 1974.
[36] Landgraf RW, Richards FD, LaPointe NR. Fatigue life predictions for a notched member under complex load histories. SAE Tech Paper 1975;750040. doi: http://dx.doi.org/10.4271/750040.
[37] Chu CC. A new incremental fatigue method. ASTM STP 2000;1389:67–78.
[38] Stefanov SH. A curvilinear integral method for multiaxial fatigue life computing under non-proportional, arbitrary or random stressing. Int J Fatigue 1993;15:467–72.
[39] Stefanov SH. The curvilinear integral method: computer realization and testing 1 (under non-roportional reversed axial force and torque). Int J Fatigue 1995;17:567–75.
[40] Stefanov SH. The curvilinear integral method: testing 2 (under non-proportional pulsating axial force and internal pressure). Int J Fatigue 1996;18:41–8.
[41] Stefanov SH, Papuga J. Damage evolution as a continuous process. In: P 2nd int. conf. mater component performance under VAL, Germany. p. 641–50.
[42] Stefanov SH, Hanselka H, Sonsino CM. Application of IDD (integration of damage differentials) for fatigue life assessment. Report No. FB-236. Darmstadt, Germany: Fraunhofer Institute LBF; 2009.
[43] Stefanov SH. Integration of damage differentials (IDD): general presentation and verification results. Int J Fatigue 2011;33:977–84.
[44] Stefanov SH. The curvilinear integral method: a question to the critical plane concept. Int J Fatigue 1997;19:101–7.
[45] Meggiolaro MA, Castro JTP, Wu H. A general class of non-linear kinematic models to predict mean stress relaxation and multiaxial ratcheting in fatigue problems – Part I: Ilyushin spaces. Int J Fatigue 2016;82:167–78.
[46] Jiang Y, Sehitoglu H. Modeling of cyclic ratchetting plasticity, Part I: Development of constitutive relations. J Appl Mech 1996;63:720–5.